Physico-chemical characterization and kinetic study of methylene blue adsorption onto a Moroccan Bentonite

Ikram DAOU, Omar ZEGAOUI, Rachid CHFAIRA, Hammou AHLAFI and Hamou MOUSSOUT

Research Team: Materials and Applied Catalysis, Laboratory "Chimie-Biologie Appliquées à l'Environnement", Department of Chemistry, Faculty of Sciences, Moulay Ismail University, PB. 11201 Zitoun, Meknès, Morocco

Abstract- A Moroccan Benonite taken from a geological site in the North-Eastern Rif of Morocco has been characterized by XRF, CEC measurements, XRD, IRTF, SEM and N_2 adsorption/desorption at -196 °C. The results showed that the structure of the purified bentonite (PB) is constituted exclusively of monmorillonite and some Mg^{2+} and Fe^{3+} cations replace Al^{3+} in the octahedral sheet. The specific surface area developed is of 74 m^2 g^{-1}, and the diameters of pores are superior to 38 Å indicating the presence of mesopores. The adsorption study of methylene blue (MB) onto PB showed that the percentage removal of this molecule can reach 99.6%, and the amount of MB adsorbed depends closely on adsorbent dosage, pH and solution temperature. The results of the adsorption tests showed that the experimental data fitted very well the pseudo second order model. Also, it was found that for temperatures ≤ 45 °C, the adsorption process proceeds by surface adsorption followed by an internal diffusion into the particles with Ea=49.7 kJ.mol-1; while for temperatures ≥ 55 °C, it is governed by an internal diffusion into the particles with Ea = 2.3 $kJ.mol^{-1}$. The low Ea values are characteristic of physical adsorption.

Index Terms- Moroccan Bentonite, Montmorillonite, Adsorption kinetics, Methylene Blue, Pseudo second order model, Intra-particle diffusion

I. INTRODUCTION

This article guides a stepwise walkthrough by Experts for writing a successful journal or a research paper starting from inception of ideas till their publications. Research papers are highly recognized in scholar fraternity and form a core part of PhD curriculum. Research scholars publish their research work in leading journals to complete their grades. In addition, the published research work also provides a big weight-age to get admissions in reputed varsity. Now, here we enlist the proven steps to publish the research paper in a journal.

The textile industries produce a large amount of wastewater fraught with dyes that pollute the aquatic environment. To reduce the negative impact of these pollutants on the environment, this wastewater must be treated before being discharged into rivers. The commonly used methods for dyes removal are biological oxidation, photochemical degradation, chemical oxidation and adsorption on materials [1-8]. The latter has been found to be one of the most efficient physicochemical processes [9]. Adsorption techniques have been conducted successfully in removing color dyes species using various adsorbents such as coal fly ash [10], solid agricultural wastes [11], and clays [12,13]. However, in recent years clays have attracted great interest because of their important physicochemical properties giving it high sorption ability even for the heavy organic molecules [14]. One of the important properties of clays (e.g. montmorillonite) is that the layers are negatively charged and this negative charge is balanced by hydrated cations placed in the interlayer species leading to high attraction towards cationic dyes, like Methylene Blue. This dye molecule has been largely used as probes to characterize clays [12,15] The objectives of this work are, on the one hand, the investigation of the physico-chemical of a natural bentonite taken from a geological site in the North-Eastern Rif of Morocco (Region of Nador). On the other hand, the kinetics studies of methylene blue adsorption onto this bentonite.

Experimental

II.1. Bentonite samples

The Bentonite samples used in this work belong to the same batch of raw natural bentonite taken from a geological site in the North-Eastern Rif of Morocco. Its purification consists in ridding it of all crystalline phases (quartz, feldspar, Calcite, etc) and retaining only well-defined size fractions, those of less than 2 microns. Typically, 100 mg of raw bentonite were dispersed in 500 mL of distilled water and kept under constant agitation for 1 hour. The suspension was transferred to a burette with a capacity of 500 ml and left to precipitate for 10 min. The collected fraction is the one corresponding to 2 cm from the height of the upper limit. It was then centrifuged for 10 min 5000 revolutions per minute (rpm) and dried overnight in an oven at 100 °C. The chemical analysis of the raw and purified samples of Bentonite was carried out using an Axios Sequential X-ray Fluorescence Spectrometer (XRF). The cation exchange capacity (CEC) was determined using a method based on cobaltihexamine chloride absorbance [16,17]. The X-ray diffraction (XRD) patterns of adsorbents were determined with an X'PERT MPD_PRO diffractometer using Cu Kα radiation at 45 kV and 40 mA over the range (2θ) of 4-70º. The determination of the crystalline phases was carried out by applying the Bragg law where λ = 1.5406 Å. FTIR spectra (400-4000 cm^{-1}) were recorded on a JASCO 4100 spectrophotometer. The samples were prepared in KBr discs from highly dried mixtures of 4% (weight/weight) and stored in desiccators. The size and morphology of the solids obtained were observed by scanning electron microscopy (SEM) (Quanta 200 from FEI Company). N_2 adsorption/desorption measurements at -196 °C were performed using an ASAP 2010. The specific surface area and the average pore diameter were determined according to the standard Brunauer-Emmett-Teller (BET) and Barrett, Joyner and Halenda (BJH) methods, respectively. The pH_{pzc} was determined at 25 °C following a

method based on conductometric titration and described in our previous work [18].

II.2. Chemicals and reagents

Methylene Blue (MB), used in this work as adsorbate, was obtained from Fisher Scientific International Company. $[Co(NH_3)_6]Cl_3$ was purchased from Sigma Aldrich Company and specified to be ≥ 99.5% purity. Bi-distilled water was used in all experiments.

II.3. Adsorption studies

The adsorption kinetic studies were conducted in a batch reactor at different temperatures (25, 35, 45, 55 and 65 °C) in a thermoregulated system to vary the temperature in the reactor between 25 and 100 °C. All the experiments were carried out at a constant speed of 500 rpm. Working solutions of MB were prepared from the stock solution (10^{-3} mol/L) to the desired concentrations for each experimental run. For all the experiments, 50 mg of purified bentonite (PB) sample was added into a 50 mL of unbuffered MB solution (pH ≈ 5.6) at desired concentration and temperature. At the end of the adsorption period, the solution was filtered under vacuum by using a filtration system equipped with micro-porous filter (0.45 µm). The dye concentration was estimated spectrophotometrically by using a UV/Vis spectrophotometer (Shimadzu 2100 spectrophotometer) at λ_{max}= 662 nm, corresponding to the maximum absorbance of MB. The amount of MB adsorbed on the PB sample in each time (q_t) was calculated according to the following mass balance equation:

$$q_t = (C_0 - C_t)\frac{V}{m} \quad (1)$$

where C_0 was the initial dye concentration (mg/L), C_t its concentration (mg/L) at time t (min), V the solution volume (L) and m the amount of PB sample used (g).

Results and discussion

III.1. Physico-chemical characterization

Chemical analysis of raw and purified bentonite are shown in Table I. It appears that the purification of the bentonite reduces the amount of silica, alumina, and Na^+, K^+ and Ca^{2+} cations; however, the amount of Fe_2O_3 and MgO increases. This indicates that a part of the quantity of Fe and Mg is contained in the clay network by substituting Al^{3+} by Fe^{3+} and/or by Mg^{2+}. The CEC obtained for the purified bentonite is of 88.82 meq/g.

Table I: Chemical analysis (%) and CEC (meq/g_{PB}) of raw and purified bentonite.

Sample	SiO_2	Al_2O_3	Fe_2O_3	MgO	Na_2O	K_2O	CaO	OO[a]	LI[b]	CEC (meq/g)
Raw Bentonite	56.15	24.23	1.85	2.04	3.08	0.75	1.21	1.39	9.30	-
Purified Bentonite	54.80	18.00	6.00	5.15	1.75	0.25	0.35	3.50	10.20	88.82

a: Other oxides in trace
b: Loss on ignition at 900°C

In order to check the structure of raw and purified bentonite, XRD analysis was carried out. Figure. 1 shows the XRD patterns of (a) raw and (b) purified bentonite. It shows that raw bentonite displays peaks belonging to the montmorillonite structure (denoted M) [19,20] quartz (denoted Q) [20] and cristobalite (denoted C) [20] as well as other unidentified peaks (denoted U) which belong to impurities in trace amounts. Indeed, the spectrum b corresponding to the purified sample shows peaks belonging exclusively to the montmorillonite structure.

The infrared spectra recorded for raw (a) and purified bentonite (b) are evident in the wavenumber range 400-4000 cm^{-1} and are presented in Figure 2. The broad absorption band around 3430 cm^{-1} and the band at 1640 cm^{-1} appearing in the two spectra are due to the stretching and bending vibrations respectively of H_2O adsorbed on the surface and between the interlayer [21-24]. The band at 3630 cm^{-1} can be ascribed to the stretching vibration of hydroxyl group in different environments (Al,AlOH), (Al,MgOH) or (Al,FeOH) [21-26]. This suggests that Al^{3+} cations are partially substituted by Mg^{2+} and /or Fe^{3+} cations. This is supported by the presence of the band at 915 cm^{-1} and the shoulder 880 cm^{-1} associated with the bending vibration of the OH group in (Al,Al)-OH and (Al,Fe)-OH respectively [21-27]. The shoulder near 3240 cm^{-1} observed on the two spectra can be ascribed to an overtone of the bending mode of cation hydration water [21,22,24]. Also, we note the presence of an intense broadband centered at 1038 cm^{-1} that can be assigned to the Si-O vibration of the tetrahedral sheet [21,22,28].

The shoulder near 1115 cm^{-1} is attributed to the vibration of Si-O in an amorphous network of SiO_2 [26]. The absorption band at 624 cm^{-1} is related to the perpendicular vibration of the octahedral cations (R-O-Si) where R = Al, Mg or Fe [20]. The band at 530 cm^{-1} is attributed to the bending vibration of Si-O in Si-O-Al [22,24,28]. The band 459 cm^{-1} is assigned to Si-OFe and/or Si-OAl vibrations [28].

SEM images show that the raw (Figure 3A) and purified (Figure 3B) bentonite samples are composed of homogeneous particles in the form of sheets characteristic of clays. No change in the morphology of the samples can be observed after purification.

Figure 4A shows that the N_2 adsorption/desorption isotherm at -196 °C recorded for PB sample belongs to the type IV isotherms according to the IUPAC nomenclature [29]. This type of isotherm is characteristic for materials that contain aggregated planar particles forming slit shape pores. Such result is in accordance with the literature data [25,29]. The adsorption at small values of P/P_0 is an indication of the existence of micropores. At higher relative pressure ($P/P_0 \geq 0.4$), clear hysteresis loop of the H2 type appears. The calculated specific area using the BET method [29] is of 74 m^2 g^{-1}. The pores diameter distribution was obtained using the BJH method from the desorption isotherm (Figure 4B). It shows that the diameters

of pores are superior to 38 Å indicating the presence of mesopores. The total pore volume is 0.09168 $cm^3 g^{-1}$.

The determined pH_{pzc} using the method based on conductometric titration [18] is of 9.2±0.2.

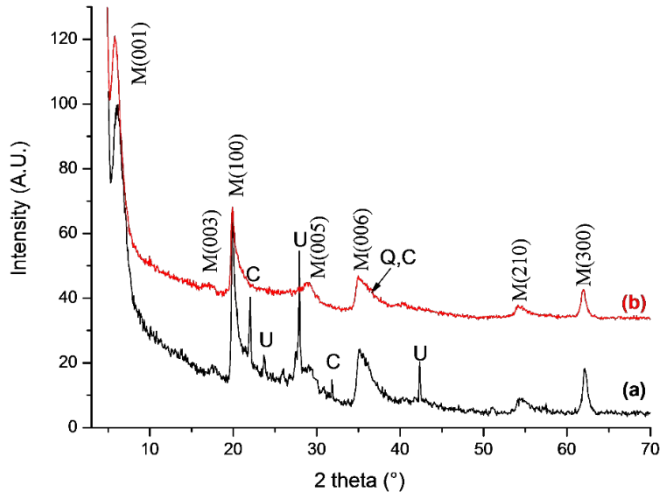

Figure 1: XRD patterns of (a) raw and (b) purified bentonite.
M: Montmorillonite. Q: Quartz. C: Cristobalite. U: unidentified

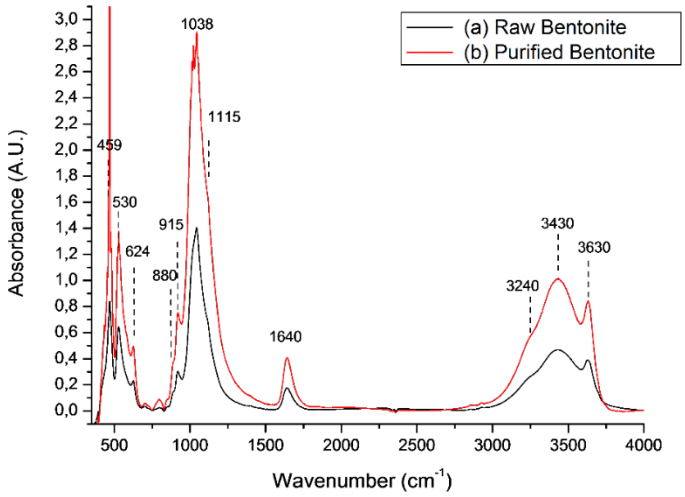

Figure 2: Infrared spectra of (a) raw and (b) purified bentonite.

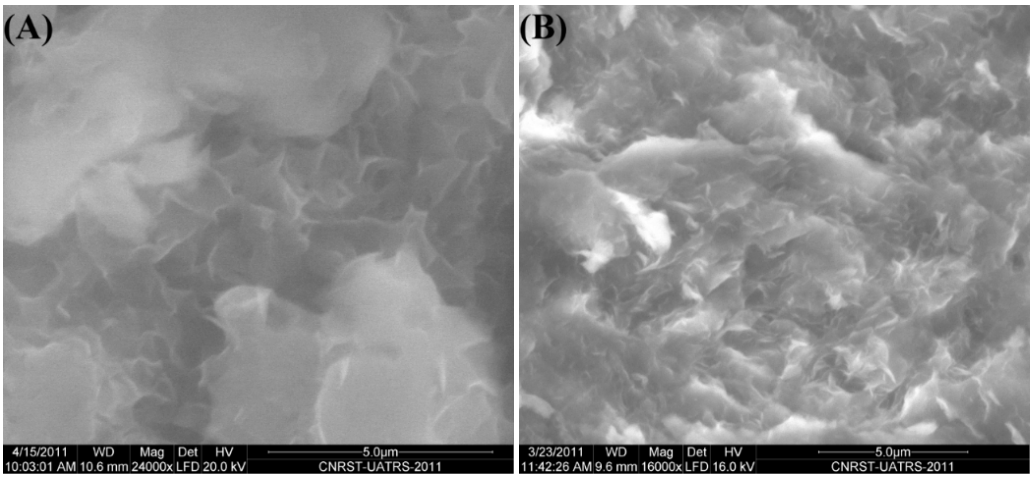

Figure 3: SEM micrographs of (A) raw and (B) purified bentonite.

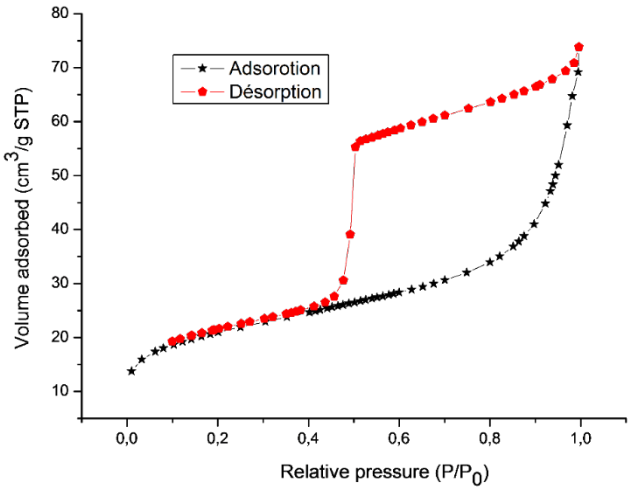

Figure 4A: Nitrogen adsorption/desorption isotherm at -196 °C.

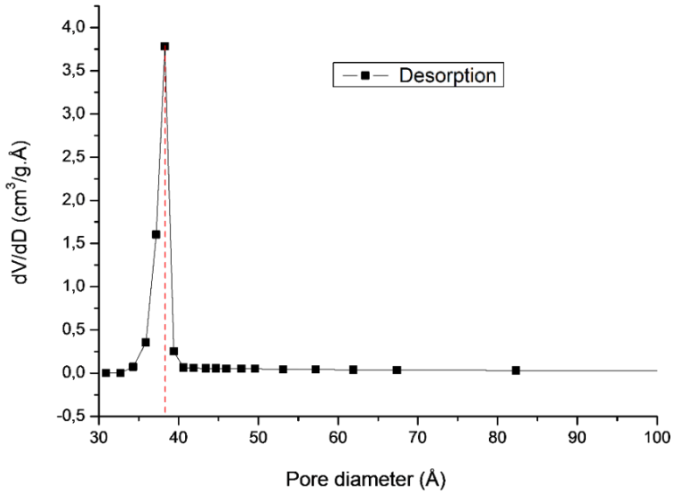

Figure 4B: Pores diameter distribution of purified bentonite particles.

III.2. Kinetic study

III.2.1. Effect of contact time and temperature

The effect of contact time on the adsorption of MB onto PB was studied at five temperatures at different times. Figure 5 shows that the required time in order that no adsorption of MB on PB sample takes place at 25 °C is seven hours. Nevertheless, the adsorption equilibrium is reached more rapidly when the temperature increases from 25 to 65 °C (adsorption equilibrium is reached in 60 min at 65 °C) indicating an increase in the rate of diffusion of the adsorbate molecules across the external boundary layer and in the internal pores of the adsorbent particles [30]. The removal of methylene blue increases slightly from 297 to 312 mg/g by increasing the temperature of the solution from 25 to 65 °C indicating the process to be endothermic.

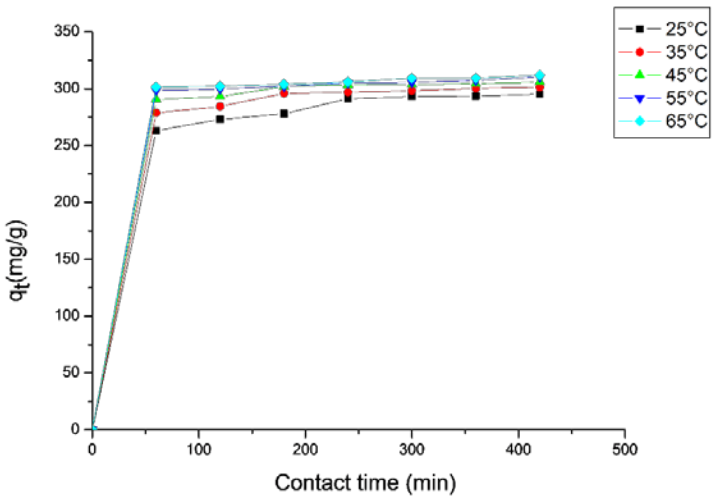

Figure 5: Effect of contact time on the adsorption of MB onto PB at different temperatures. $C_{0(MB)}$ = 10^{-3} mol/L ; pH = 5.6 ; m_{PB} = 50 mg.

III.2.2. Effect of adsorbent concentration

The effect of PB concentration on MB adsorption at a contact time of 7 hours was studied by varying the bentonite dose from 0.4 to 4 g/L. The volume of the solution was kept constant (50 mL). Figure 6 shows that the amount of methylene blue adsorbed at equilibrium decreases from 377.8 to 79.6 mg/g, while the percentage of removal of MB increases from 47.2 to 99.6% for an increase in adsorbent concentration from 0.4 to 4 g/L. At adsorbent doses between 1.5 and 4 g/L, the percentage of removal of MB changes slightly. This indicate that the more the adsorbent dosage, the larger the volume of effluent that a fixed mass of purified bentonite can purify. The decrease in amount of dye adsorbed q_e (mg/g) with increasing adsorbent mass is due to the split in the flux or the concentration gradient between MB concentration in the solution and in the adsorbent surface. Thus with increasing adsorbent mass, the amount of dye adsorbed onto unit weight of adsorbent gets reduced. Similar results have been obtained by many authors for the adsorption of methylene blue on monmorillonite clay [31] and rice husk [32], and for the adsorption of Congo red on acid activated red mud [33].

III.2.3. Effect of pH

The variation of the amount of MB adsorbed at equilibrium onto PB was investigated as a function of initial suspension pH ($2 \leq pH \leq 10$). The pH was adjusted using diluted solutions of NaOH or HCl. Figure 7 shows the extent of dye adsorption at different pHs. From this figure, it was observed that the amount of MB adsorbed at equilibrium onto PB increases from 178 to 280 mg/g with the increasing of pH of dye solution from 2 to 8, and then declines slightly to 274 mg/g for pH = 10. Whereas, the percentage of removal of MB increases continuously from 69.7 to 99.5% with increasing pH of MB solution from 2 to 10 indicating that the basic solution was advantageous to MB adsorption onto PB. It is clear that the solution pH influences profoundly the adsorption process as reported by many authors [31,34,35]. The pH_{pzc} determined in this work for purified bentonite is of 9.2. Consequently, for pH< 9.2, the number of negatively charged adsorbent sites decreases and the number of positively charged surface sites increases with decreasing the pH solution in the range 8-2. Then, electrostatic repulsion prevents the adsorption of cationic molecules such as MB^+ [35,36]. Also, lower adsorption of methylene blue at acidic pH can be attributed to the presence of excess H^+ ions competing with dye cations for the adsorption sites [35].

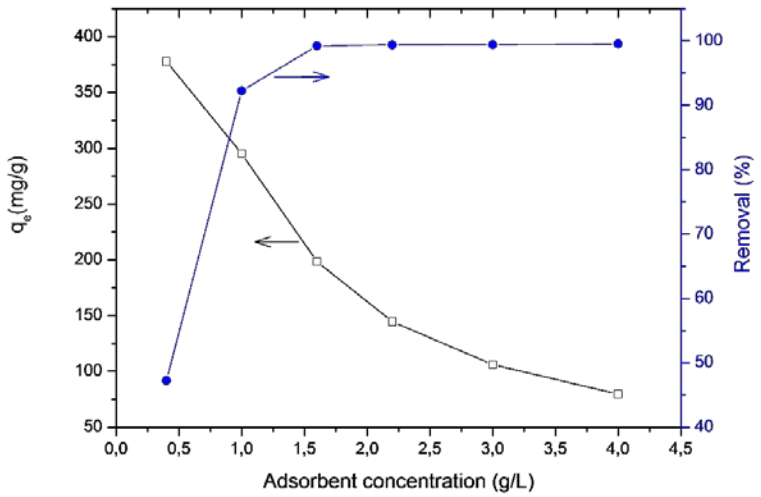

Figure 6: Effect of PB concentration on MB adsorption at equilibrium.
C_0(MB) = 10^{-3} mol/L ; pH = 5.6 ; V_{sol} =50 mL ; contact time = 7h ; T = 25°C.

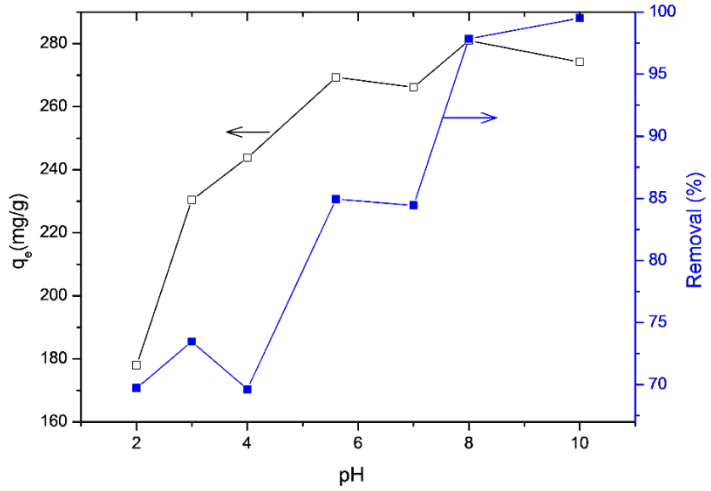

Figure 7: Effect of initial suspension pH on the adsorption of MB onto PB.
C_0(MB) = 10^{-3} mol/L ; m_{PB} = 50 mg ; V_{sol} =50 mL ; contact time = 7 h ; T = 25 °C.

II.3. Adsorption kinetics

The adsorption kinetic of MB onto PB was studied by applying pseudo first order (Eq. (2) [37]), pseudo second order (Eq. (3) [38]) and intra-particle diffusion (Eq. (4) [39]) models to the experimental data.

$$Ln(q_e - q_t) = Lnq_e - k_1 t \quad (2)$$

$$\frac{t}{q_t} = \frac{1}{k_2 q_e^2} + \frac{t}{q_e} \quad (3)$$

$$q_t = k_i t^{0.5} + C \quad (4)$$

where q_e (mg/g) and q_t (mg/g) are the amount of MB adsorbed onto PB at equilibrium and at time t (min) of adsorption process respectively; k_1 (min^{-1}), k_2 (g mg^{-1} min^{-1}) and k_i (mg g^{-1} $min^{-0.5}$) are the pseudo first order, pseudo second order and intra-particle diffusion rate constants respectively and C is the intercept.

III.3.1. Intra-particle diffusion model

Figure 8 shows the plot between q_t versus $t^{0.5}$ for MB onto PB at different solution temperature and C_0(MB) =10^{-3} M. From this figure, it was found that the sorption process seems to follow one or two steps depending on solution temperature. For temperatures ≤ 45 °C, the two phases observed in the intra-particle diffusion plots suggest that the adsorption of MB onto PB proceeds certainly by surface adsorption followed by an internal diffusion into the particles. For temperatures ≥ 55°C, the plots of q_t versus $t^{0.5}$ show a single straight indicating that the adsorption of MB onto PB proceeds by an internal diffusion into the particles. This behavior can be attributed to the existence of a large amount of mesopores in the sample conjugated to the solubility of MB that increases with increasing solution temperature. On the other hand, intra-particles plots do not pass

through the origin indicating that other processes can control the rate of adsorption simultaneously with intra-particles diffusion [34]. The k_i values calculated from the slopes of the second linear portion [32] (for T ≤ 45°C) and the intercepts are given in Table 2. Generally, the intercept values calculated (Table 2) increase with the increasing of solution temperature.

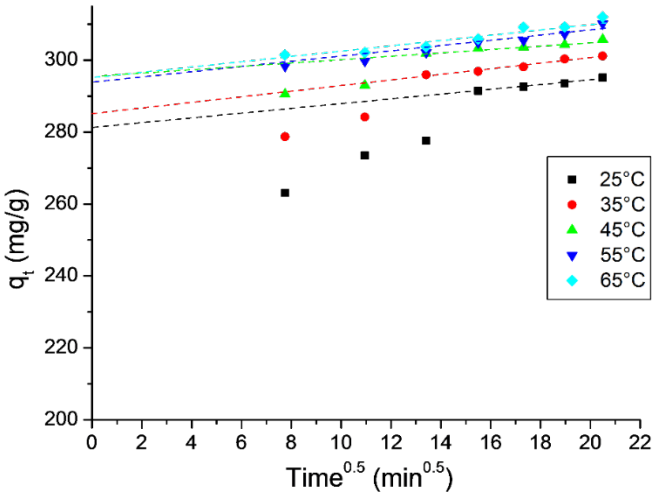

Figure 8: Intra-particle diffusion plot for MB onto PB at different solution temperature. C_0(MB) = 10^{-3} mol/L; mPB = 50 mg; Vsol = 50 mL; pH = 5.6 (natural).

Table 2: Kinetic values calculated at different temperatures for methylene blue adsorption onto purified bentonite. C_0(MB) = 10^{-3} mol/L; m_{PB} = 50 mg; Vsol = 50 mL; pH = 5.6 (natural).

		Pseudo first order			Pseudo second order			Intra-particle diffusion		
T (°C)	q_e[(a)] (mg.g^{-1})	k_1 (min^{-1})	q_e[(b)] (mg.g^{-1})	R^2	k_2 (g.mg^{-1}.min^{-1})	q_e[(b)] (mg.g^{-1})	R^2	k_i (g.mg^{-1}.min$^{0.5}$)	R^2	C[(c)]
25	297	0.0105	117.0	0.950	0.00048	298.5	0.9996	0.7722	0.959	281.2
35	303	0.0101	87.3	0.919	0.00078	304.0	0.9998	0.7855	0.968	285.4
45	307	0.0103	83.5	0.892	0.00116	306.8	0.9999	0.4952	0.947	294.6
55	311	0.0098	71.5	0.878	0.00120	309.6	0.9999	0.7996	0.949	294.0
65	312	0.0148	114.4	0.866	0.00122	311.5	0.9999	0.9222	0.932	294.0

(a) and (b) : the experimental and calculated q_e values respectively
(c) : the intercept values

III.3.2. Pseudo first order and pseudo second order models

In order to investigate the mechanism of adsorption, the pseudo first order and pseudo second order kinetics model were used to test the experimental data. The coefficients of determination and the pseudo first order rate parameters as well as the pseudo second order rate parameters are shown in Table 2. On the basis of q_e and R^2 values obtained for the two kinetic models, it is clear that the experimental data fit very well the pseudo second order model. Indeed, the calculated $q_{e,2}$ values are very close to those obtained experimentally and the coefficients of determination for the pseudo second order kinetic model are very close to 1 indicating the applicability of the kinetic Eq. (3) expressing the pseudo second order nature of the adsorption process of methylene blue onto purified bentonite. Similar results have been reported for the adsorption of methylene blue onto perlite [30] and monmorillonite clay [31]. Also, Table 2 shows that k_2 increases with the increasing of solution temperature which is consistent with a physisorption [39].

III.4. Activation parameters

The activation energy was calculated from the linearized Arrhenius equation (Eq. (5)) and the pseudo second order rate constants obtained at different temperatures.

$$\mathrm{Ln}k_2 = \mathrm{Ln}A - \frac{E_a}{RT} \quad (5)$$

where k_2 is the pseudo second order rate constant (g mg^{-1} min^{-1}), A the temperature independent Arrhenius factor (g mg^{-1} min^{-1}), Ea the activation energy (J mol^{-1}), R the gas constant (J mol^{-1} K^{-1}) and T the solution temperature (K).

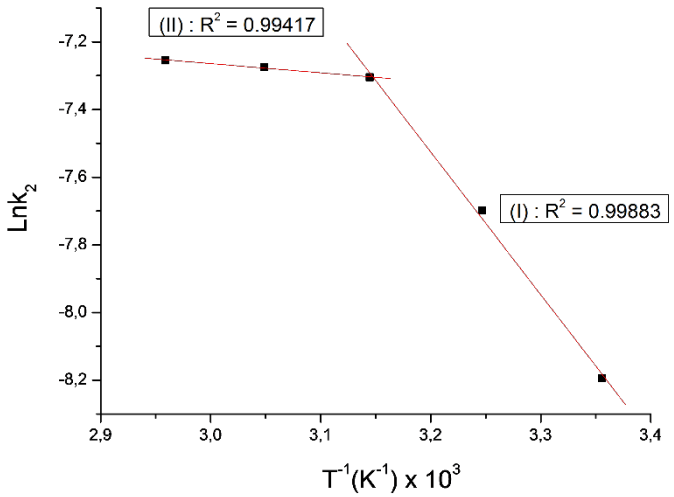

Figure 9: Arrhenius plot for adsorption of MB onto PB.
C_0(MB) = 10^{-3} mol/L ; m_{PB} = 50 mg; V_{sol} = 50 mL; pH = 5.6 (natural).

As shown in Figure 9, the plot of Lnk_2 vs T^{-1} gives two straight lines with a good coefficient of determination. The Ea values calculated from the slopes are 49.7 and 2.3 kJ mol^{-1} for the straight lines (I) and (II) respectively. This behavior suggests that the sorption process of MB onto PB proceeds by two different mechanisms depending on solution temperature. These results confirm those obtained previously. For temperatures ≤ 45°C, the adsorption process is certainly governed by surface adsorption followed by an internal diffusion into the particles. The value of Ea (49.7 kJ mol^{-1}) is characteristic of physical adsorption [40]. For temperatures > 45°C, the very low value of obtained Ea (2.3 kJ mol^{-1}) corresponds, also, to physisorption [40] and indicates that the rate is controlled by intra-particle diffusion mechanism [40,41].

II. CONCLUSION

The bentonite sample collected in Nador region was characterized using different techniques as XRF, CEC measurements, X-ray diffraction, infrared spectroscopy, SEM observations and N_2 adsorption/desorption measurements at -196 °C. The results show that the crystalline structure of purified bentonite is exclusively constituted of monmorillonite and some Mg^{2+} and Fe^{3+} cations replace Al^{3+} in the octahedral sheet.

The adsorption and kinetic studies show that:

- The MB adsorption equilibrium is reached in approximately seven hours at 25 °C and one hour at 65 °C. The removal percentage of MB can reach 99.6% and the amount of the adsorbed dye depends closely on adsorbent dosage, pH solution and solution temperature.

- A comparison of the kinetic models showed that the MB sorption onto PB was described very well by the pseudo second order rate model. It was also found that for temperatures ≤ 45 °C, the adsorption of MB onto PB proceeds certainly by surface adsorption followed by an internal diffusion into the particles with activation energy of 49.7 kJ mol^{-1}. While for temperatures ≥ 55 °C, the adsorption process proceeds by an internal diffusion into the particles with activation energy of 2.3 kJ mol^{-1}. This behavior is consistent with the description of the sorption process as involving physisorption and two different mechanisms depending on solution temperature.

REFERENCES

[1] S.M. Ghoreishi, R. Haghighi, Chem. Eng. J. 95 (2003) 163-169.
[2] A.K. Jain, V. K Gupta, A. Bhatnagar, Suhas. J. Hazard. Mater. B101 (2003) 31-42.
[3] Y.S. Ho, G. McKay, Process Biochem. 38 (2003) 1047-1061.
[4] F. Derbyshire, M. Jagtoyen, R. Andrews, A. Rao, I. Martin-Gullon, E. Grulke, L.R. Radovic (Eds.), In Chemistry and Physics of Carbon, New York, Marcel Dekker, 2001, pp. 1-66, Vol. 27.
[5] Y. Zhiyong, D. Laub, M. Bensimon, J. Kiwi, Inorg. Chim. Acta. 361 (2008) 589-594.
[6] M. Qamar, M. Saquib, M. Muneer, Dyes. Pigments. 65 (2005) 1-9.
[7] C. Namasivayam, R. Yamuna, T. Jayanthi, J. Cell. Chem. Technol. 37 (2003) 333-339.
[8] R. Dhodapkar, N.N. Rao, S.P. Pande, S.N. Kaul, Bioresource Technol. 97 (2006) 877-885.
[9] V.K. Gupta, A. Mittal, L. Kurup, J. Mittal, J. Colloid. Interf. Sci. 304 (2006) 52-57.
[10] J.X. Lin, S.L. Zhan, M.H. Fang, X.Q. Qian, H. Yang, J. Environ. Manage. 87 (2008) 193-200.
[11] B.H. Hameed, R.R. Krishni, S.A. Sata, J. Hazard. Mater. 162 (2009) 305-311.
[12] A. Gürses, Ç. Doğar, M. Yalçın, M. Açıkyıldız, R. Bayrak, S. Karaca, J. Hazard. Mater. B131 (2006) 217-228.
[13] M.Y. Teng, S.H. Lin, Desalination. 201 (2006) 201 71-81.
[14] C. Bilgiç, J. Colloid. Interf. Sci. 281 (2005) 33-38.
[15] G. Rytwo, C. Serban, S. Nir, L. Margulies, Clay. Clay Miner. 39 (1991) 551-555.
[16] D. Aran, A. Maul, J.F. Masfaraud, C.R. Geoscience. 340 (2008) 865-871.
[17] F. Favre, D. Tessier, M. Abdelmoula, J.M. Génin. W.P. Gates. P. Boivin, Eur. J. Soil. Sci. 53 (2002) 175-183.
[18] I. Daou, R. Chfaira, O. Zegaoui, Z. Aouni, H. Ahlafi, Mediteer. J. Chem. 2 (2013) 569-582.
[19] A. Viani, A.F. Gualtieri, G. Artioli, Am. Mineral. 87 (2002) 966-975.

[20] Z.P. Tomić, V.P. Logar, B.M. Babic, J.R. Rogan, P. Makreski, Spectrochi. Acta A. 82 (2011) 389-395.
[21] V.C Farmer, In Infrared Spectra of Minerals. Mineralogical Society. Farmer, V.C. Eds. London, UK, 1974.
[22] J. Madejová, Vib. spectrosc. 31 (2003) 1-10.
[23] V.S. Somerset, L.F. Petrik, R.A. White, M.J. Klink, D. Key, E. Iwuoha, Talanta. 64 (2004) 109-114.
[24] J.T. Kloprogge, E. Mahmutagic, R.L. Frost, J. Colloid Interf Sci. 296 (2006) 640-646.
[25] P. Bankovic´, A.M. Nikolic´, Z. Mojovic´, N.J. Jovicic´, M. Perovic´, V. Spasojevic´, D. Jovanovic´, Micropor. Mesopor. Mat.165 (2013) 247-256.
[26] Z. Vukovic´, A. Milutonovic´, L. Rožić,; A. Rosić, Z. Nedić, D. Jovanović, Clay. Clay Miner. 54 (2006) 697-702.
[27] V.C. Farmer, J.D. Russell, Clay Clay Miner. 15 (1967) 121-142.
[28] F. Ayari, E. Srasra, M.T. Ayadi, Desalination. 185 (2005) 391-397.
[29] S.G. Gregg, K.S.W. Sing, Adsorption. Surface Area and Porosity, 2nd Eds Academic Press, London, 1982.
[30] M. Doğan, M. Alkan, A. Türkyilmaz, Y. Özdemir, J. Hazard. Mater. 109 (2004) 141-148.
[31] C.A.P.Almeida, N.A. Debacher, A.J. Downs, L. Cottet, C.A.D. Mello, J. Colloid. Interf. Sci. 332 (2009) 46-53.
[32] V. Vadivelan, K.V. Kumar, J. Colloid. Interf.Sci. 286 (2005) 90-100.
[33] A. Tor, Y. Cengeloglu, J. Hazard. Mater. 138 (2006) 409-415.
[34] Y. Seki, K. Yurdakoç, Adsorption 12 (2006) 89-100.
[35] O. Hamdaoui, J. Hazard. Mater. B135 (2006) 264-273.
[36] S. Chandrasekhar, P.N. Pramada Adsorption12 (2006) 27-43.
[37] S. Lagergren, B.K. Svenska,Vetenskapsakademiens Handlingar 24 (1898) 1-39.
[38] Y.S. Ho, G. McKay, Chem. Eng. J. 70 (1998) 115-124.
[39] S. Tunali, A.S. Özcan, A. Özcan, T. Gedikbey, J. Hazard. Mater. 135 (2006) 141-148.
[40] M. Doğan, M. Alkan, Ö. Demirbas, Y. Özdemir, C. Özmetin, Chem. Eng. J. 124 (2006) 89-101.
[41] M. Doğan, M. Alkan, Y. Onganer, Water Air Soil Poll. 120 (2000) 229-248.

AUTHORS

First Author –Ikram DAOU, PhD student, Research Team: Materials and Applied Catalysis, Laboratory “Chimie-Biologie Appliquées à l’Environnement “, Department of Chemistry. Faculty of Sciences, Moulay Ismail University, PB. 11201 Zitoun, Meknès, Morocco, Ikram.chimie@gmail.com

Second Author – Omar ZEGAOUI, Professor, Research Team: Materials and Applied Catalysis, Laboratory “Chimie-Biologie Appliquées à l’Environnement“, Department of Chemistry. Faculty of Sciences, Moulay Ismail University, PB. 11201 Zitoun, Meknès, Morocco ozegaoui@gmail.com

Third Author – Rachid CHFAIRA, Professor, Research Team: Materials and Applied Catalysis, Laboratory “Chimie-Biologie Appliquées à l’Environnement“, Department of Chemistry. Faculty of Sciences, Moulay Ismail University, PB. 11201 Zitoun, Meknès, Morocco, chfaira65@gmail.com.

Fourth Author – Hammou AHLAFI, Professor, Research Team: Materials and Applied Catalysis, Laboratory “Chimie-Biologie Appliquées à l’Environnement“, Department of Chemistry. Faculty of Sciences, Moulay Ismail University, PB. 11201 Zitoun, Meknès, Morocco, hahlafi@yahoo.fr.

Fifth Author – Hamou MOUSSOUT, PhD student, Research Team: Materials and Applied Catalysis, Laboratory “Chimie-Biologie Appliquées à l’Environnement“, Department of Chemistry. Faculty of Sciences, Moulay Ismail University, PB. 11201 Zitoun, Meknès, Morocco, moussouthammou@gmail.com

Correspondence Authors – Ikram DAOU, Email: ikram.chimie@gmail.com, Phone: +212 6 56 51 89 02. Or Omar ZEGAOUI, Email: ozegaoui@gmail.com